

**Are your MRI contrast agents cost-effective?**

Learn more about generic Gadolinium-Based Contrast Agents.



**FRESENIUS  
KABI**

caring for life

**AJNR**

**Sinonasal psammomatoid ossifying fibromas: CT and MR manifestations.**

M H Han, K H Chang, C H Lee, J W Seo, M C Han and C W Kim

*AJNR Am J Neuroradiol* 1991, 12 (1) 25-30

<http://www.ajnr.org/content/12/1/25>

This information is current as  
of April 10, 2024.

# Sinonasal Psammomatoid Ossifying Fibromas: CT and MR Manifestations

Moon Hee Han<sup>1</sup>  
Kee Hyun Chang<sup>1</sup>  
Chul Hee Lee<sup>2</sup>  
Jeong Wook Seo<sup>3</sup>  
Man Chung Han<sup>1</sup>  
Chu-Wan Kim<sup>1</sup>

Five cases of pathologically proved psammomatoid ossifying fibromas of the sinonasal area are presented. All five cases were examined by CT and in three cases MR imaging was performed before and after injection of gadopentetate dimeglumine. The lesions were located in the sphenothmoidal area and extended over the nasal cavity or orbit in four cases. In one case, the lesion occurred at the perpendicular plate of the ethmoid bone with preservation of the ethmoidal sinus. On CT, all the lesions were expansile and circumscribed by a thick bony wall. Internal septations of bone density (four cases) or enhancing soft-tissue density (one case) were seen and internal content was low in density in all but one from which blood was aspirated. On MR, the bony walls were isointense with gray matter on T1-weighted images and were seen as areas of low intensity on T2-weighted images. The lesions significantly enhanced after injection of contrast material.

A well-circumscribed multiloculated expansile mass with a thick wall of bone density on CT scans and enhancement of this area on postcontrast MR images is strongly suggestive of psammomatoid ossifying fibroma.

*AJNR* 12:25-30, January/February 1991

Ossifying fibroma, a rare, slowly growing tumor arising in the nasal cavity, is one of many benign fibroosseous lesions of the craniofacial area [1-3]. Differentiation from other forms of fibroosseous lesion, especially fibrous dysplasia, is important because of the different course and prognosis. Fibrous dysplasia is a disease with a self-limiting clinical course, and surgery is rarely indicated, while ossifying fibroma is a progressively growing tumor in which surgical resection is needed. Differentiating the two conditions is difficult at times because of partial radiologic and histologic similarity. Some reports [1, 4-6] emphasize the importance of radiologic findings in differentiating between these entities in the mandible, indicating that fibrous dysplasia fails to exhibit well-demarcated borders whereas ossifying fibromas are well-demarcated and amenable to surgical excision. In sinonasal ossifying fibroma, there are scattered descriptions [7-9] of CT features and, to our knowledge, no MR findings were reported. This study presents the CT and MR findings of five pathologically proved cases of psammomatoid ossifying fibroma of the sinonasal area.

## Materials and Methods

We reviewed five CT scans and three MR images of five patients with pathologically proved sinonasal psammomatoid ossifying fibroma. The three males and two females were 12-56 years old; their clinical and radiologic findings are summarized in Table 1. All patients presented with symptoms of a local mass, such as exophthalmos or facial swelling. One patient (case 5) had a history of partial resection of a mass about 1 year earlier. CT was performed with a GE 9800 CT scanner (GE Medical Systems, Milwaukee) after contrast injection, and both axial and coronal images were obtained with 3- or 5-mm thickness in all patients. Three

Received April 5, 1990; revision requested May 21, 1990; revision received September 5, 1990; accepted September 7, 1990.

Presented at the annual meeting of the American Society of Neuroradiology, Los Angeles, March 1990.

<sup>1</sup> Department of Diagnostic Radiology, Seoul National University College of Medicine, Seoul 110-744, Korea. Address reprint requests to M. H. Han.

<sup>2</sup> Department of Otolaryngology, Seoul National University College of Medicine, Seoul 110-744, Korea.

<sup>3</sup> Department of Pathology, Seoul National University College of Medicine, Seoul 110-744, Korea.

0195-6108/91/1201-0025

© American Society of Neuroradiology



patients (cases 3, 4, 5) underwent MR imaging on a 0.5-T superconducting unit (Supertec 5000, Goldstar, Seoul, Korea) with cylindrical surface coil before and after contrast (Magnevist, Schering AG, Berlin, W. Germany) injection (0.1 mmol/kg). Axial T2-weighted, 2000/40,85/2 (TR/TE excitations), spin-echo images and T1-weighted, 500/30/4, images were obtained before injection of contrast material. After enhancement, only T1-weighted images were obtained in both axial and coronal planes. The slice thickness was 6 mm with a 2-mm interslice gap, and the field of view as 200 mm with a  $256 \times 200$  matrix in all pulse sequences. All five patients underwent surgical resection and in two patients (cases 1 and 5) the second resection was done 1 year after the first because of recurrence. CT and MR findings were analyzed and compared.

## Results

The locations of the lesions were sphenoethmoidal in three cases and orbitofrontoethmoidal and nasosphenoidal in one

case each. The lesions protruded into the orbit causing proptosis in four cases. In one patient (case 1) the mass was located at the mid-nasal cavity with the preservation of both ethmoidal air cells, suggesting the perpendicular plate of the ethmoid as the site of origin (Fig. 1). The sizes of the lesions were 5–10 cm in the longest diameter.

On CT, all tumors had thick shells of bone density outlining the lesions with irregular internal and smooth external surfaces. The lesions were completely covered by these shells in all but one patient (case 4), in whom there was focal disruption of the shell (Fig. 2). Multiloculated appearance of the lesion was shown in all cases. The internal septa were seen as bone density with varying thickness (Fig. 3) in three patients and as thin soft-tissue density in two patients (cases 3 and 4) (Fig. 4). The densities of each compartment were different in three patients (cases 1, 3, 4). In one of them (case

TABLE 1: Summary of Five Patients with Sinonasal Psammomatoid Ossifying Fibromas

Case No.	Age (years)	Sex	Clinical Findings		CT and MR Findings					
			Sinus(es) Involved	Presenting Symptoms	Bony Shell	Septations	CT Density of Content	Enhancement on MR	Signal Intensity of Shell (T1/T2)	Signal Intensity of Content (T1/T2)
1	21	M	Sphenoidal, nasal cavity	Nasal obstruction	Smooth and complete	Multiple and calcified	Hypo- and isodense			
2	56	M	Ethmoidal, orbitofrontal	Exophthalmos	Irregular and complete	Multiple and calcified	Isodense			
3	12	F	Ethmoidal, sphenoidal, nasal cavity	Exophthalmos	Smooth and complete	Single and not calcified	Hypo- and isodense	Homogeneous in shell	↓/↓	→/↑ (med) ↑/↑ (lat)
4	21	F	Ethmoidal, sphenoidal, nasal cavity	Exophthalmos	Irregular with focal disruption	Multiple and partly calcified	Hypo- and isodense	Heterogeneous in shell and septa	→/↓	↓/↑
5 <sup>a</sup>	16	M	Ethmoidal, sphenoidal	Exophthalmos	Irregular and complete	Multiple and calcified	Hypo- and hyperdense	Heterogeneous in shell and septa	→/↓	↓/↑

Note.—SI = signal intensity; ↑ = hyperintense; → = isointense; ↓ = hypointense; med = medial compartment; lat = lateral compartment.

<sup>a</sup> Case 5 had partial resection of a nasal mass 1 year before present study.

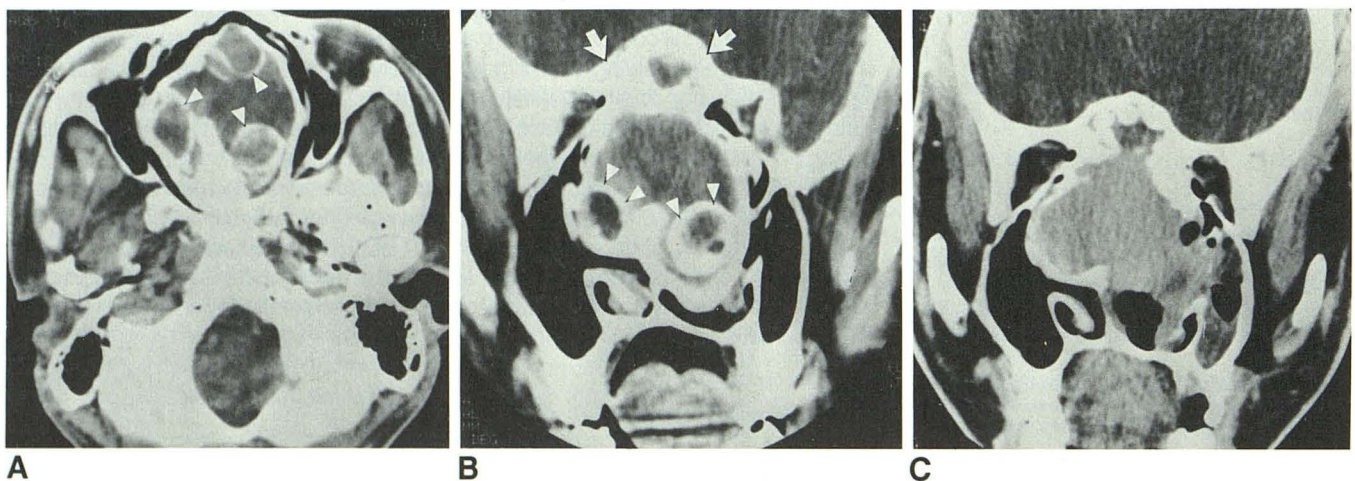


Fig. 1.—Case 1: 21-year-old man with nasal obstruction.

A and B, Preoperative axial (A) and coronal (B) CT scans show large mass involving nasal cavity and sphenoid bone with multiloculated appearance in lower portion (arrowheads). The mass was demarcated by a thick shell of bone density in the sphenoid area (arrows in B).

C, Coronal CT scan 1 year after resection shows recurrent nasal mass with homogeneous soft-tissue density and no intratumoral calcification or septation.



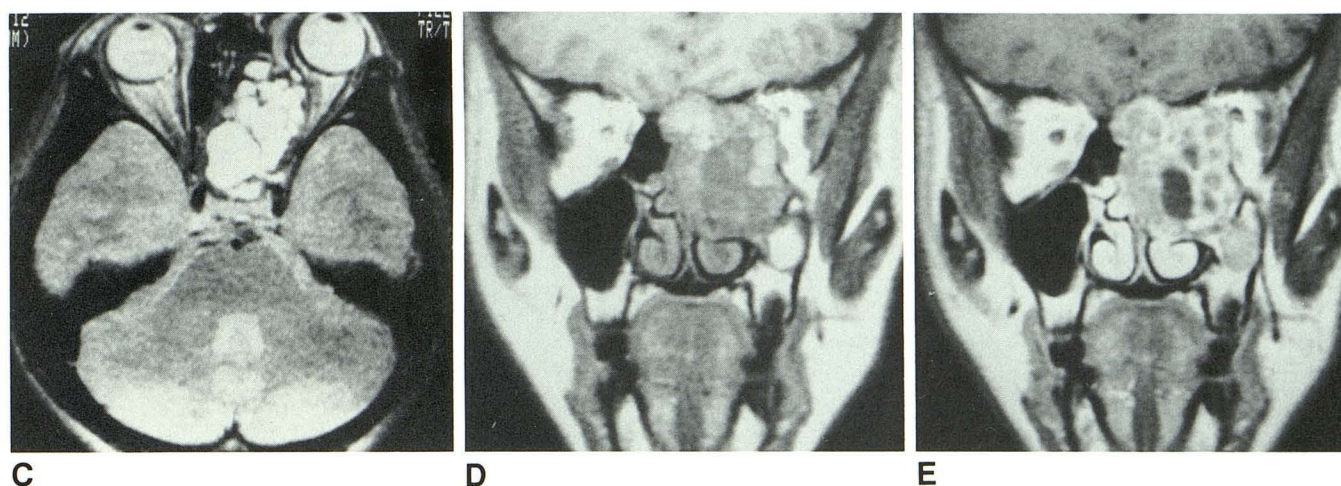
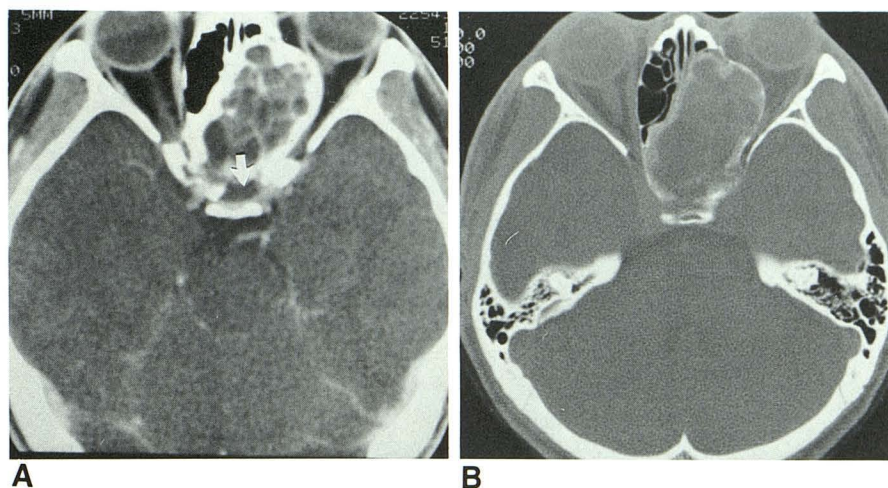


Fig. 2.—Case 4: 21-year-old woman with exophthalmos.

A, Axial CT scan at mid-orbit level shows multiseptated mass with a thick bony shell involving the left ethmoidal and sphenoidal sinuses. Note focal disruption of bony shell (arrow) with extension of mass into pituitary fossa, suggesting local aggressiveness of the tumor.

B, Thin-slice axial CT scan with bone windows shows abnormal bone of tumor as lower density than normal bony structure.

C–E, Outer shell is seen as area of low intensity on T2-weighted MR image, 2000/85 (C), as area of isointensity on precontrast T1-weighted image (500/30) (D), and as area of hyperintensity on postcontrast T1-weighted image, 500/30 (E).

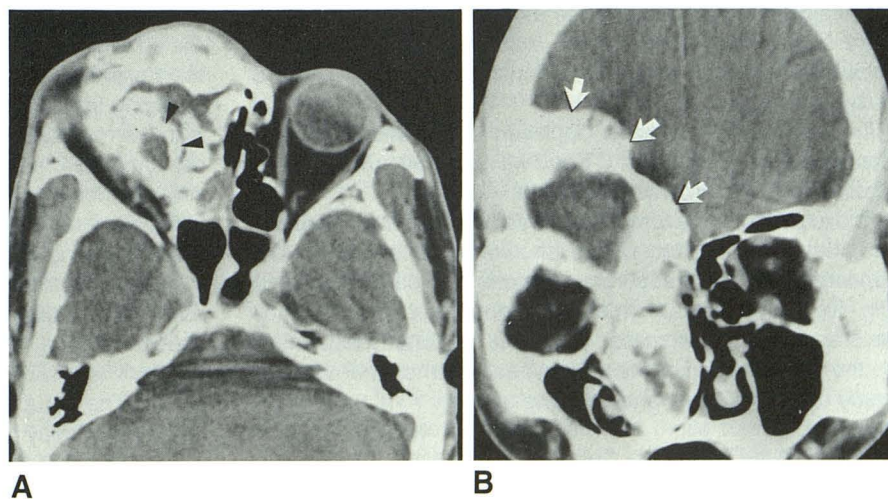


Fig. 3.—Case 2: 56-year-old man with painless frontal swelling and exophthalmos.

A, Axial CT scan of mid-orbit level shows large heavily calcified mass in right ethmoidal sinus bulging into right orbit. Multiloculation of mass by thick walls of bone density are shown (arrowheads).

B, Coronal CT scan shows large intracranial component of mass involving the frontal bone. Note thick shell of bone density (arrows) and homogeneous density of its content.



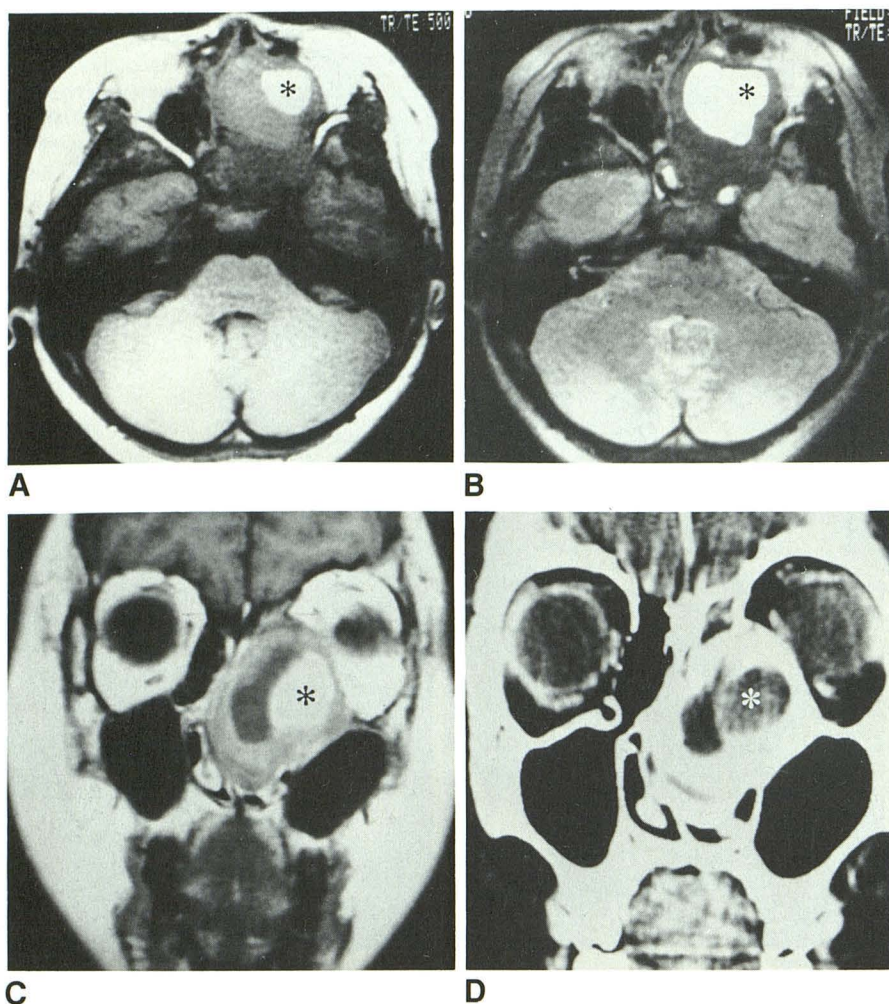


Fig. 4.—Case 3: 12-year-old girl with exophthalmos. The mass, involving ethmoid and nasal cavity, has three components on MR and CT.

A and B, Precontrast MR images. Lateral compartment of mass (asterisk) from where the blood was aspirated is shown as area of high intensity on T1-weighted image, 500/30 (A), and was not separated from medial compartment, which is another necrotic portion, on T2-weighted image, 2000/85 (B).

C, Postcontrast MR image. Thick shell of mass enhanced after injection of gadopentetate dimeglumine.

D, On CT scan, density of lateral compartment (asterisk) is higher than that of medial compartment, and outer shell is seen as bone density.

3) high density was demonstrated in a smaller compartment of the lesion and, on MR, the intensities were high on both T1- and T2-weighted images (Fig. 4). In this patient, a significant amount of venous blood was aspirated from this compartment before resection. The MR signal intensities of the shells were similar to the gray matter of brain on precontrast T1-weighted images and were low on T2-weighted images. After injection of gadopentetate dimeglumine, the enhancement of the thick shells, which were not identified on CT because of masking by the bone density, were demonstrated in all three cases.

Involved structures were displaced or expanded without any destructive change on CT and MR, indicating the expansile nature of the growth in all cases.

In two patients, the tumors recurred after subtotal resection and the recurrent tumor was shown to be similar in CT appearance to the preoperative state in one patient (case 5) (Fig. 5). In another patient (case 1), who had been shown to have a multiloculated mass with septa of bone density (Fig. 1), the recurrent tumor was shown as a homogeneous soft-tissue density within a shell of bone density.

## Discussion

The benign fibroosseous lesions of jaw and facial bone constitute a diverse group of conditions, including fibrous

dysplasia, ossifying fibroma, florid osseous dysplasia, focal sclerosing osteomyelitis, and osteitis deformans [10, 11]. These lesions may share common microscopic features of hypercellular fibroblastic vascular stroma with a variety of calcified matrices represented by woven bone, lamellar bone, curvilinear trabeculae, and sphenoid calcifications [1, 10].

Psammomatoid ossifying fibroma is a tumor that is not related to dental structure. This lesion frequently occurs in the ethmoid or orbit in young people, and has been referred to in previous publications as ossifying fibroma [3], juvenile ossifying fibroma [12], and cementifying fibroma [13].

In the mandible, the radiologic diagnosis of psammomatoid ossifying fibroma is suggested by the findings of a well-circumscribed, expansile lesion with calcified matrices [14]. In the sinonasal area, the lesion may show somewhat different features owing to the complexity of surrounding structures. In a lesion protruding into an air-filled space, such as the nasal cavity, the margin of the mass is clearly demarcated, as shown in case 1 (Fig. 1), while the margin of the lesion adjacent to a bony structure may not be clearly demarcated on CT. The abrupt transition of bone thickness at the margin of the lesion may help to delineate the lesion and differentiate it from fibrous dysplasia, which shows poorly demarcated bone thickening on CT. With bone windows, abnormal bone of the tumor can be differentiated from surrounding bony



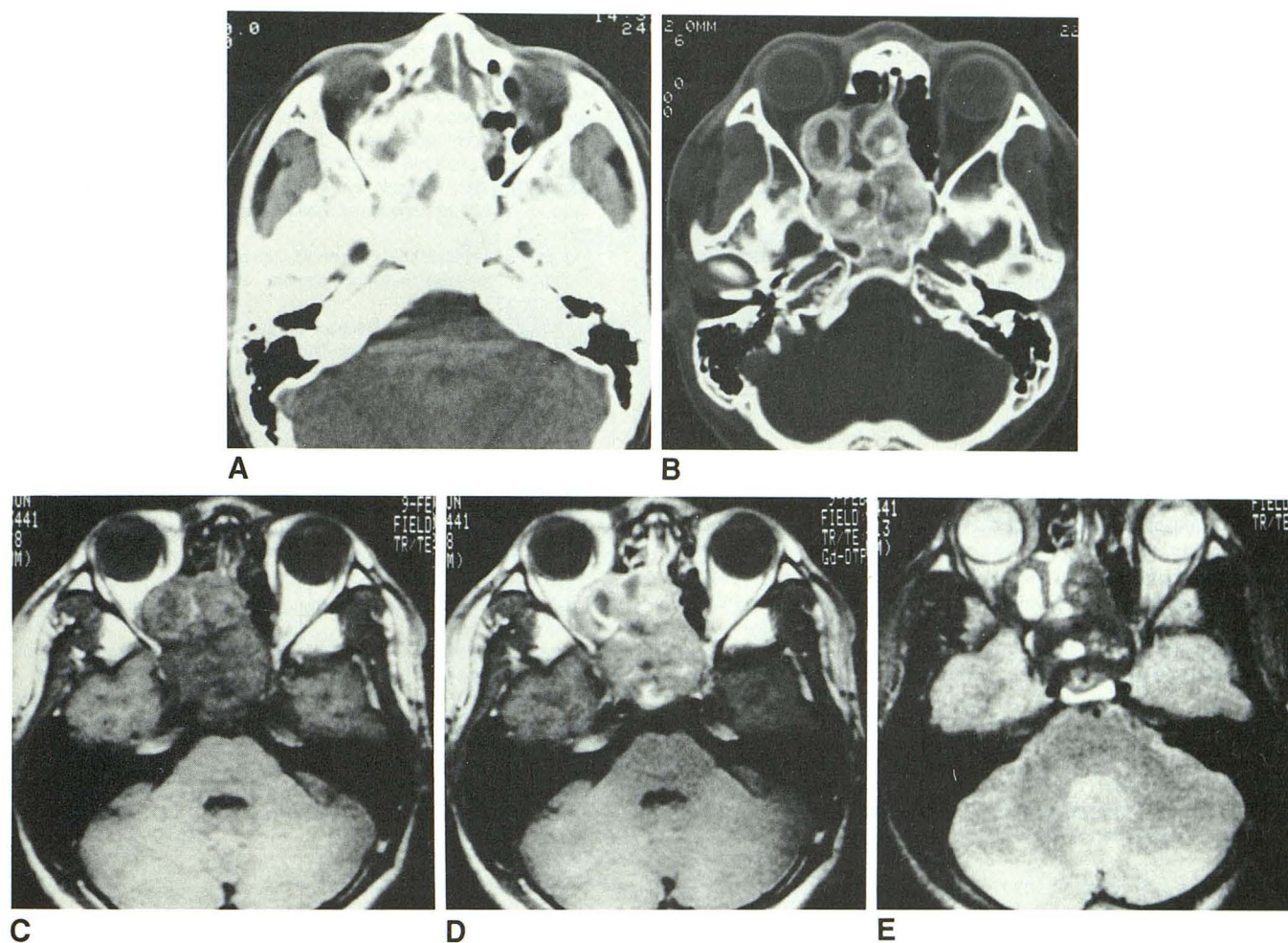


Fig. 5.—Case 5: 16-year-old boy with exophthalmos.  
 A, Preoperative CT scan shows large mass involving right ethmoidal and sphenoidal sinuses with dense calcification.  
 B, Follow-up CT scan with bone setting 1 year after subtotal resection shows recurrence of lesion, with appearance of mass similar to preoperative state.  
 C–E, Compared with precontrast image (C), postcontrast T1-weighted image, 500/30 (D), better demonstrates enhancement of mass. On T2-weighted image, 2000/85 (E), intensity of calcified portion is similar to that of muscle.

structures by CT (Fig. 2E). MR can demonstrate contrast enhancement of the bony shell (Fig. 5). This finding suggests that the thick bony shell is not a reactive hyperostosis but a tumor tissue. In two of our patients (cases 1 and 5) (Figs. 1 and 5) the tumor recurred in the partly remaining bony shell of the skull base after the first surgical resection.

In the three patients with ethmoid lesions (cases 3, 4, 5) (Figs. 3, 4, 5), the size and location were nearly the same but the internal appearance and content were quite varied. The concentration of protein in fluid content may be a possible cause of varying signal intensity of the lesion [15]. The content of the tumor is known to be a highly cellular tissue histologically [1]. However, in our series, fluid-containing spaces in the central portion of the tumor were demonstrated on MR, and surgery confirmed in one case that it was filled with blood caused by secondary hemorrhagic necrosis.

Eversole et al. [14] described the two major radiologic patterns, unilocular and multilocular, in his large series of mandibular ossifying fibromas. Unilocular lesion with radiolucency was the most prevalent pattern. In our series, all the

lesions were multilocular. Eversole et al. also stated that there was no correlation between propensity for recurrence and radiologic findings [14]. The findings of recurrent tumors in our series, which had been shown as multiloculated lesions preoperatively and as soft-tissue tumors after recurrence (Fig. 1), could not be clearly explained. The growth rate and the extent of surgery may be partly influential.

The local aggressiveness of this tumor is not unusual, especially in young patients. Some authors [4, 12, 16] have reported ossifying fibroma of the orbit and maxilla, which show aggressive growth and a tendency to recur in the juvenile age group. Different terms have been used, such as juvenile ossifying fibroma and active or aggressive ossifying fibroma, to specify the more aggressive tumor, which shows basically the same microscopic findings. Four patients in our series were juveniles or young adults, but no difference could be found in aggressiveness between these tumors and that of a patient (case 2) in the sixth decade. The location or extent of the tumor is thought to be more relevant as a surgical contraindication than as a predictor of aggressive-



ness, and complete resection of the tumor was not possible in our cases because of the large defect that would have occurred in the skull base.

In summary, sinonasal psammomatoid ossifying fibroma may show the characteristic findings on CT of a well-demarcated expansile mass covered by a thick shell of bone density with a multiloculated internal appearance and a content of varying density. Contrast-enhanced MR imaging is helpful in evaluating the extent of the tumor by showing the enhancement of the thick outer shell of the mass. With a proper clinical setting and careful analysis of CT and MR findings, one can easily diagnose this rare tumor and evaluate its extent of growth.

#### ACKNOWLEDGMENTS

We thank K. Min and H. Lim for research assistance, and S. Kong and J. Keesing for manuscript preparation.

#### REFERENCES

1. Eversole LR, Leider AS, Lelson K. Ossifying fibroma: a clinicopathologic study of sixty-four cases. *Oral Surg Oral Med Oral Pathol* **1985**;60:505-511
2. Hamner JE, Lightbody PM, Ketcham AS, Swerdlow H. Cementoossifying fibroma of the maxilla. *Oral Surg Oral Med Oral Pathol* **1968**;26:579-587
3. Lehrer HZ. Ossifying fibroma of the orbital roof. *Arch Neurol* **1969**;20:536-541
4. Fu YS, Perzin KH. Non-epithelial tumors of the nasal cavity, paranasal sinuses, and nasopharynx: a clinicopathologic study. II. Osseous and fibro-osseous lesions, including osteoma, fibrous dysplasia, ossifying fibroma, osteoblastoma, giant cell tumor, and osteosarcoma. *Cancer* **1974**;33:1289-1305
5. Small IA, Goodman PA. Giant cemento-ossifying fibroma of the maxilla: report of case and discussion. *J Oral Surgery* **1973**;31:113-119
6. Waldron CA, Giansanti JS. Benign fibro-osseous lesions of the jaws: a clinical-radiologic-histologic review of sixty-five cases. Part II. Benign fibro-osseous lesions of periodontal ligament origin. *Oral Surg* **1973**;35:340-350
7. Margo CE, Ragsdale BD, Perman KI, Zimmerman LE, Sweet DE. Psammomatoid (juvenile) ossifying fibroma of the orbit. *Ophthalmology* **1985**;92:150-159
8. Hasso AN, Vignaud J, LaMasters DL. Pathology of the paranasal sinuses, nasal cavity and facial bones. In Newton TH, Hasso AN, Dillon WP, eds. *Computed tomography of the head and neck*. New York: Raven Press, **1988**:1-7, 31
9. Som PM. Paranasal sinuses. In Taveras JM, Ferrucci JT, eds. *Radiology: diagnosis-imaging-intervention*. Philadelphia: Lippincott, **1986**:1-28
10. Waldron CA. Fibro-osseous lesions of the jaws. *J Oral Maxillofac Surg* **1985**;43:249-262
11. Reed RJ, Hagy DM. Benign nonodontogenic fibro-osseous lesions of the skull. *Oral Surg Oral Med Oral Pathol* **1965**;19:214-227
12. Damjanov I, Maenza RM, Snyder GG, Ruiz JW, Toomey JM. Juvenile ossifying fibroma: an ultrastructural study. *Cancer* **1978**;42:2668-2674
13. Khalil MK, Leib ML. Cemento-ossifying fibroma of the orbit. *Can J Ophthalmol* **1979**;14:195-200
14. Eversole LR, Merrel PW, Strub D. Radiographic characteristics of central ossifying fibroma. *Oral Surg Oral Med Oral Pathol* **1985**;59:522-527
15. Som PM, Dillon WP, Sze G, Lidov M, Biller HF, Lawson W. Benign and malignant sinonasal lesions with intracranial extension: differentiating with MR imaging. *Radiology* **1989**;172:763-766
16. Walter JM, Terry BC, Small EW, Matteson SR, Howell RM, Hill C. Aggressive ossifying fibroma of the maxilla: review of the literature and report of a case. *J Oral Surg* **1979**;37:276-286